

Supplementary Information

Mesolimbic Dopamine Reward System Hypersensitivity in Individuals with Psychopathic Traits

Joshua W. Buckholtz^{1,2}, Michael T. Treadway¹, Ronald L. Cowan³, Neil D. Woodward³, Stephen D. Benning¹, Rui Li⁴, M. Sib Ansari⁴, Ronald M. Baldwin⁴, Ashley N. Schwartzman¹, Evan S. Shelby¹, Clarence E. Smith³, David Cole⁵, Robert M. Kessler⁴, David H. Zald^{1,3}

¹Department of Psychology

²Vanderbilt Brain Institute

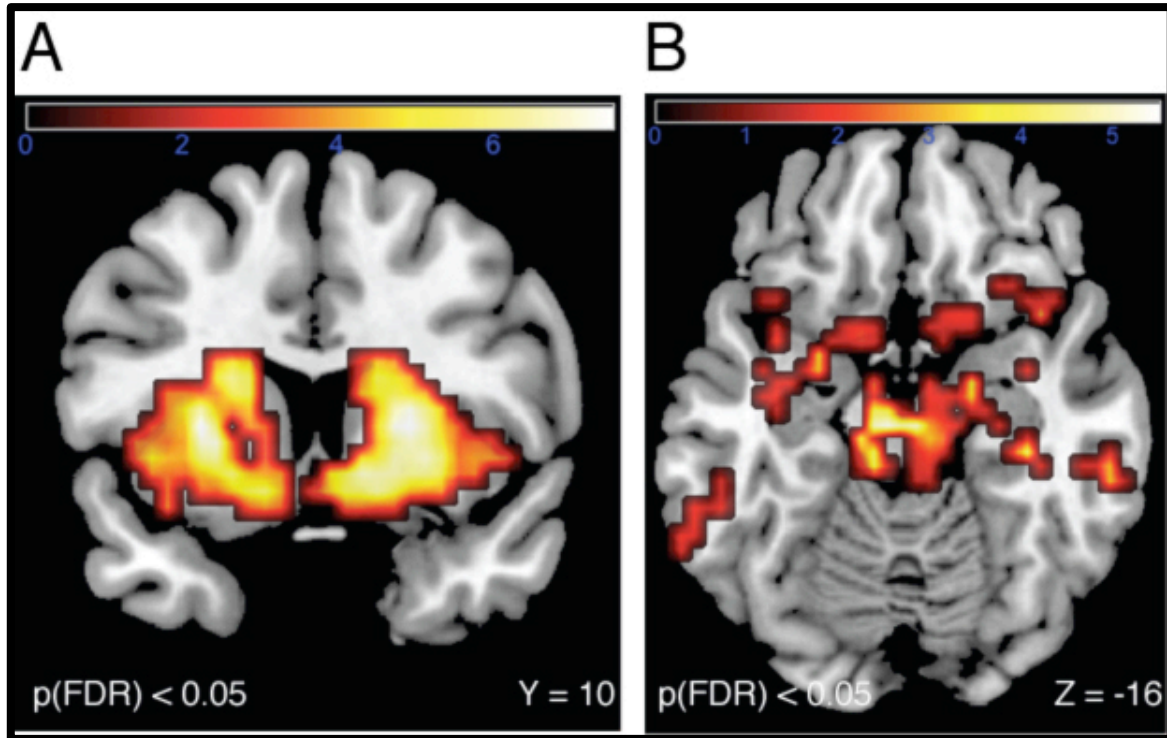
³Department of Psychiatry

⁴Department of Radiology

⁵Department of Psychology and Human Development
Vanderbilt University, Nashville, TN, 37240

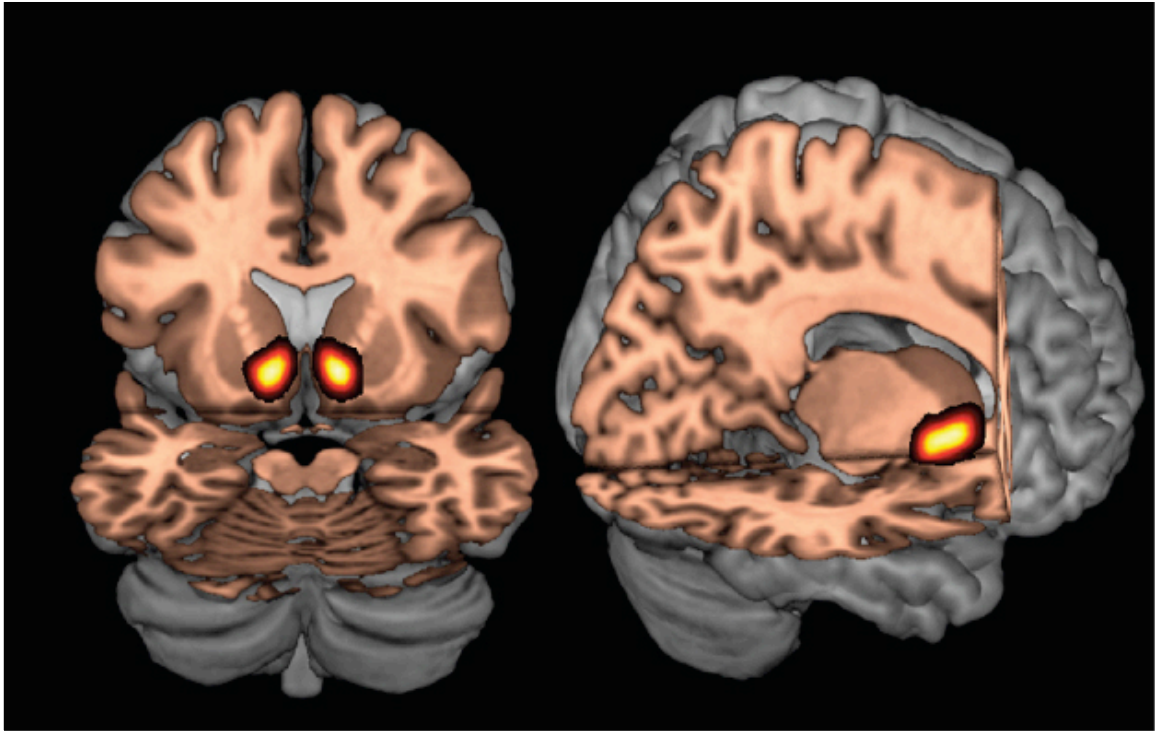
Address correspondence to: Joshua W. Buckholtz, Vanderbilt University, Department of Psychology, PMB 407817, 2301 Vanderbilt Place, Nashville, TN 37240-7817. Email: joshua.buckholtz@vanderbilt.edu. Phone: 615-343-1446

Supplementary Figures

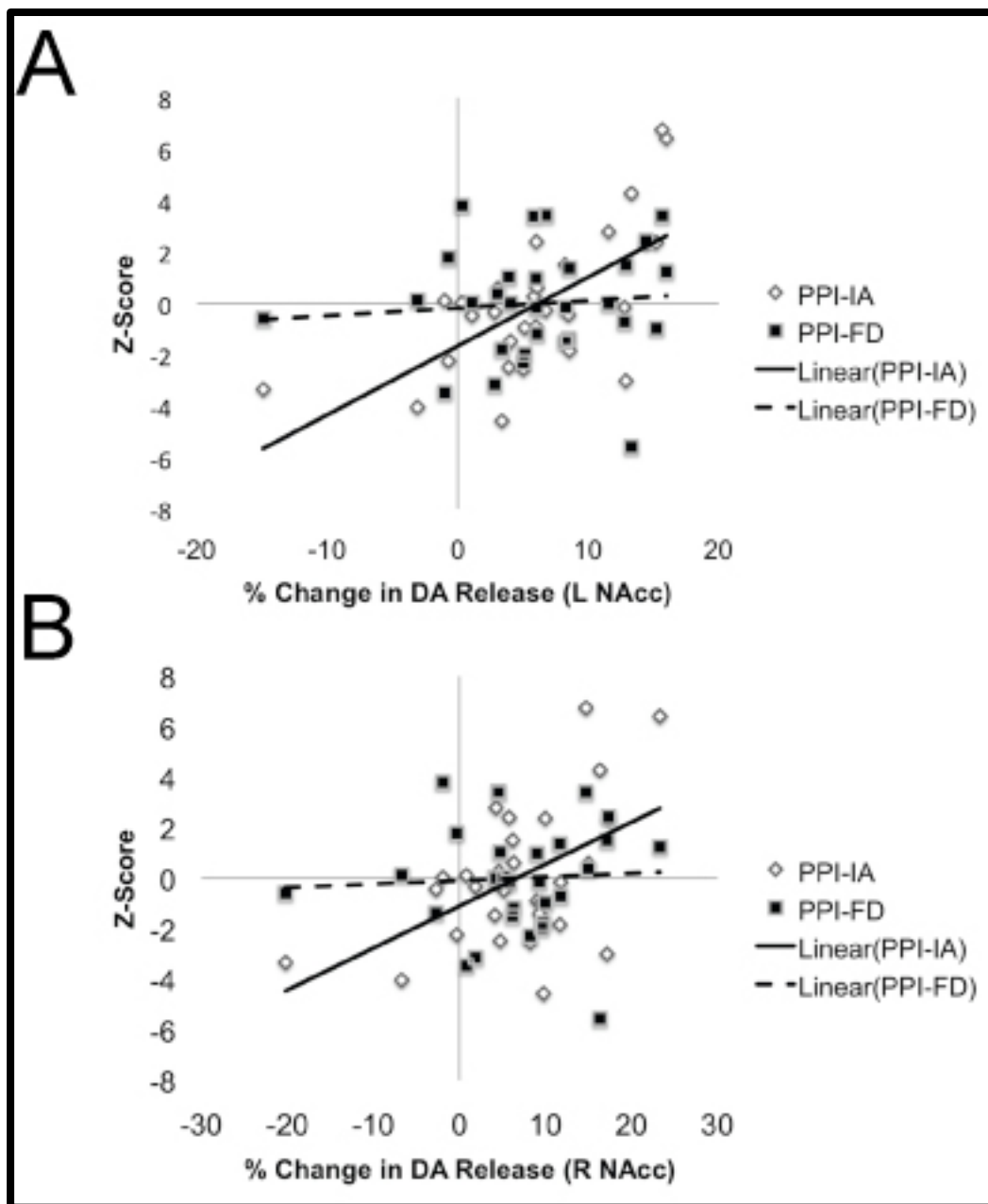


Supplementary Figure 1. Effect of amphetamine on DA release in the human brain.

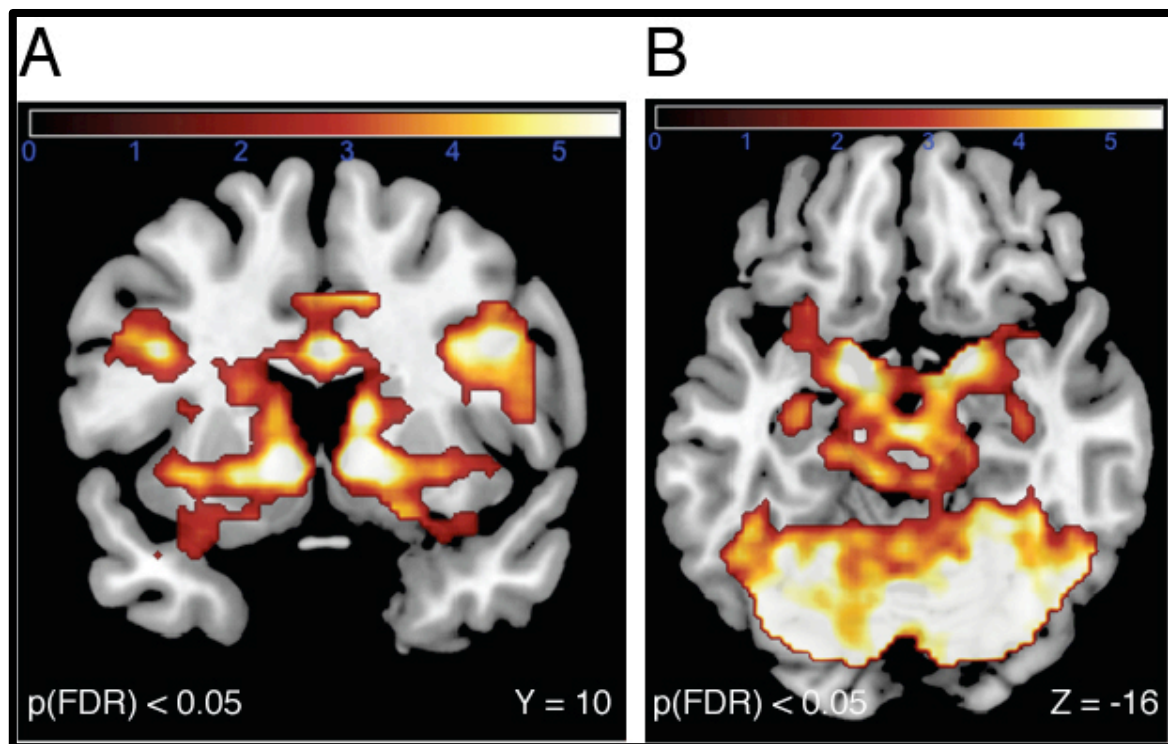
SPMs depicts the effect of amphetamine on DA release in the striatum (**A**) and in midbrain (**B**), visualized by performing a one-sample t-test on participants' placebo-corrected [^{18}F]fallypride binding potential images. Images are presented at a whole-brain threshold of $p(\text{FDR}) < 0.05$, $k > 10$). Left = Left, Right = Right. $N = 30$. Color bar indicates t-statistic value.



Supplementary Figure 2. Nucleus accumbens anatomical region of interest. Image depicts the NAcc region of interest used to mask PET and fMRI data. NAcc mask derived from the Harvard-Oxford probabilistic structural atlas.

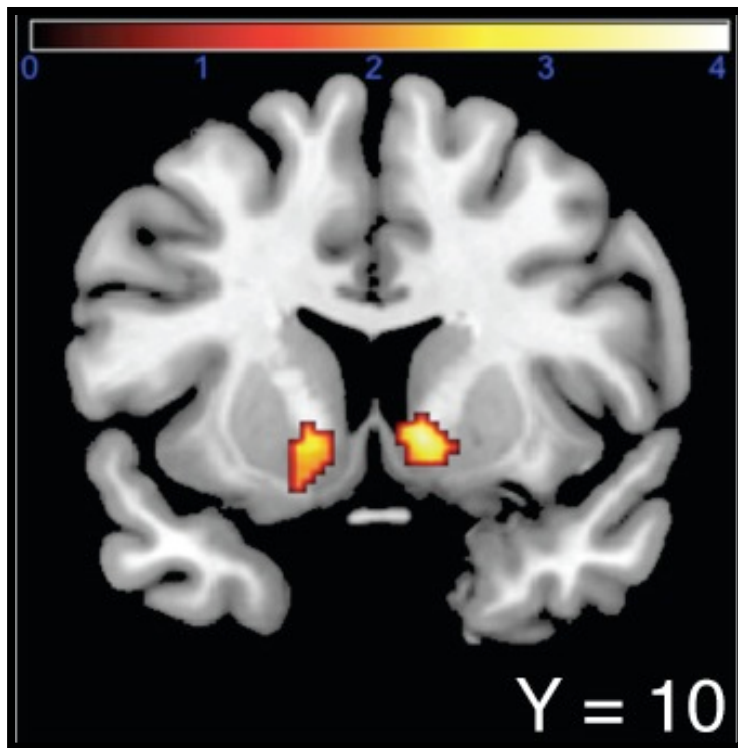


Supplementary Figure 3. PPI-IA, but PPI-FD, is associated with amphetamine-induced DA release. Scatterplots show differences in slopes for the correlations between PPI-IA, PPI-FD, and DA release in left (A) and right (B) NAcc. To avoid biasing correlation estimates, per-subject mean DA release values were calculated across entire anatomical left and right NAcc ROIs (i.e. DA release values not derived from PPI-IA correlation SPM). Right NAcc: $r = 0.51$, $p = .004$ (PPI-IA), $r = 0.05$, $p = 0.78$ (PPI-FD). Left NAcc: $r = 0.64$, $p = 0.0001$ (PPI-IA); $r = 0.09$, $p = 0.64$ (PPI-FD). Tests for dependent correlations confirm that these differences in correlations are significant (see manuscript).

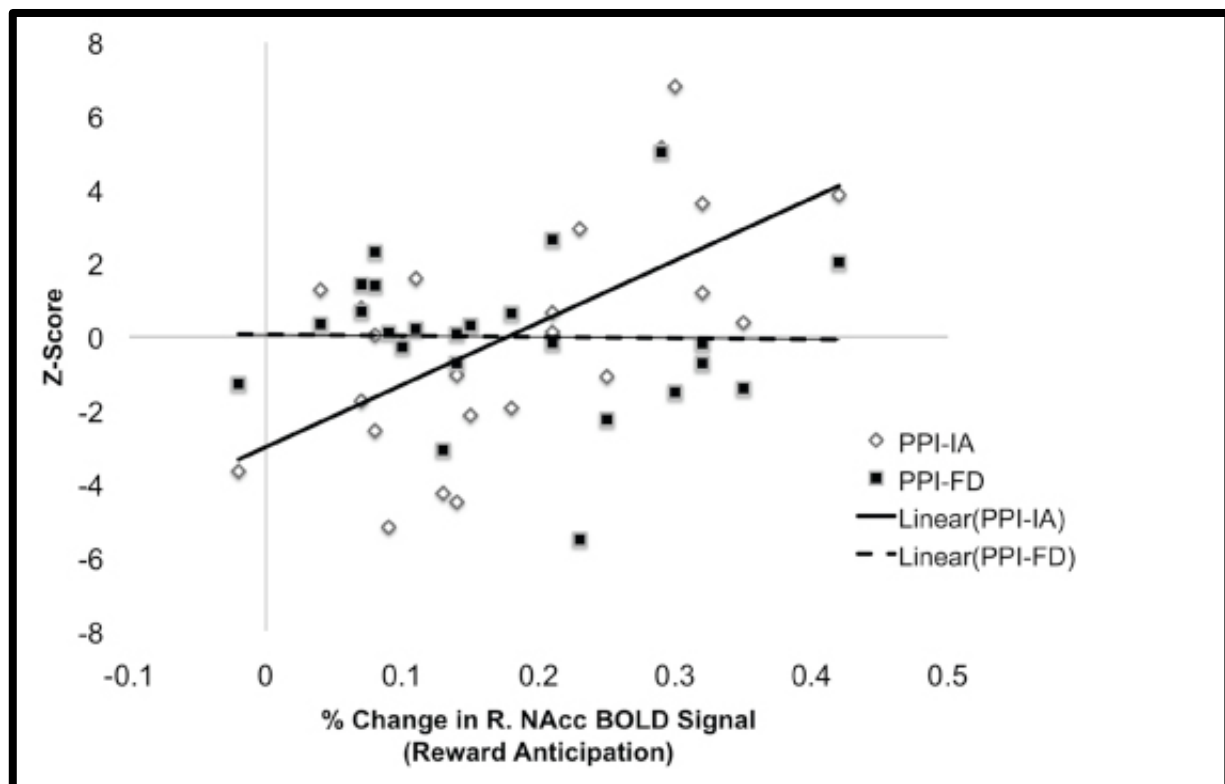


Supplementary Figure 4. Brain activation during the anticipation of monetary rewards.

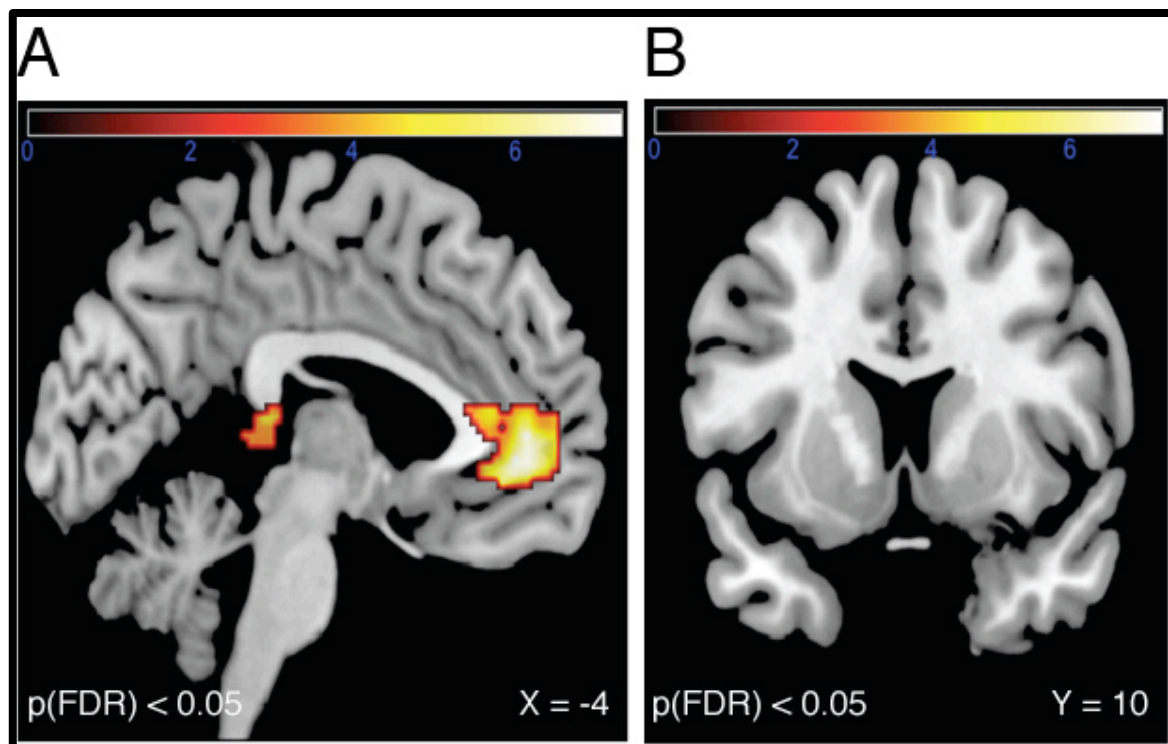
SPMs depict brain regions engaged during the anticipation of monetary rewards, visualized by performing a one-sample t-test on participants' WIN>NO CHANGE contrasts (time-locked to the onset of each trial's anticipatory phase). Images are presented at a threshold of $p(\text{FDR}) < 0.05$, $k > 10$. Left = Left, Right = Right. $N = 24$. Color bar indicates t-statistic value. Substantial activations occur in the ventral striatum, anterior cingulate, lateral prefrontal cortex, visual cortices and midbrain.



Supplementary Figure 5. PPI-IA is associated with NAcc activation during the anticipation of monetary rewards. SPM depicts a positive correlation between PPI-IA scores and NAcc BOLD signal during reward anticipation. Image masked with the Harvard-Oxford anatomical NAcc region of interest, thresholded at $p < 0.05$ (uncorrected) for visualization purposes. Left = Left, Right = Right. $N = 24$. Color bar indicates t-statistic value.

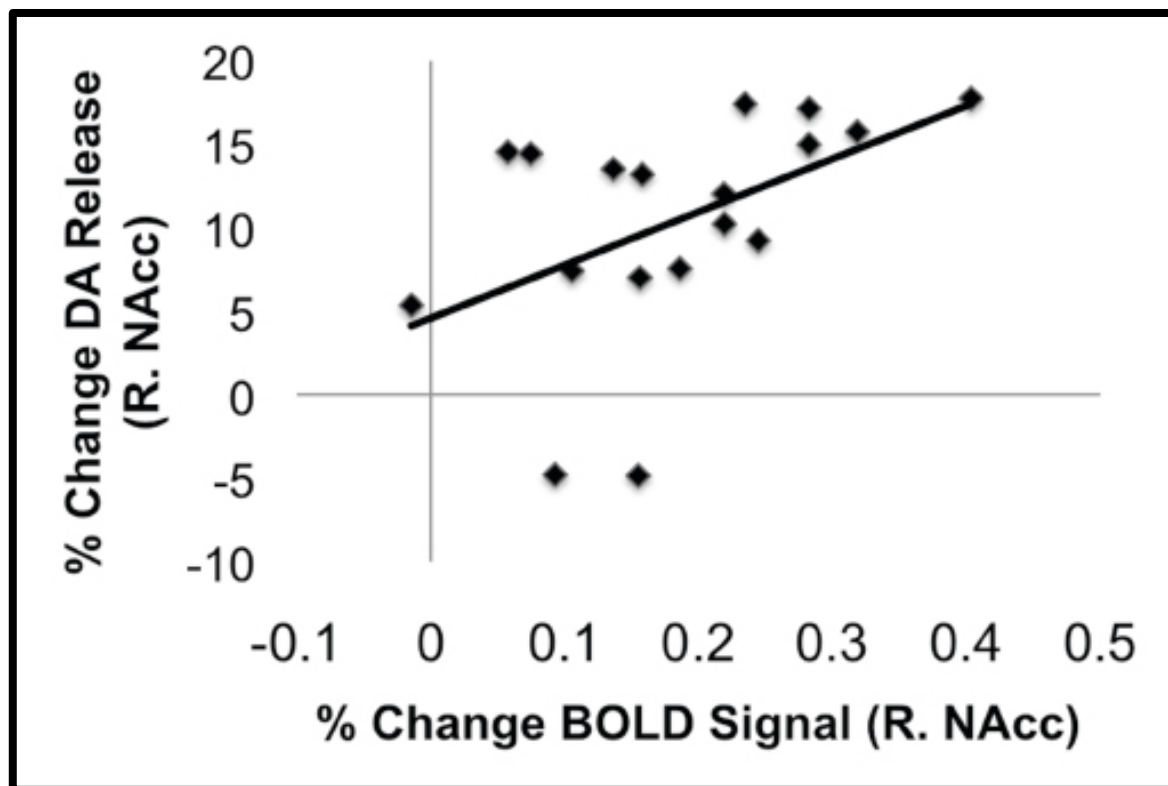


Supplementary Figure 6. PPI-IA, but not PPI-FD, is associated with NAcc BOLD signal during the anticipation of monetary reward. Scatterplots show differences in slopes for the correlations between PPI-IA, PPI-FD, and NAcc BOLD signal during reward anticipation in right NAcc. To avoid biasing correlation estimates, per-subject mean BOLD signal values were calculated across entire anatomical right NAcc ROIs (i.e. BOLD signal values not derived from PPI-IA correlation SPM). Right NAcc: $r = 0.63$, $p = 0.001$ (PPI-IA), $r = -0.02$, $p = 0.94$ (PPI-FD). Tests for dependent correlations confirm that these differences in correlations are significant (see manuscript).



Supplementary Figure 7. Brain activation during the receipt of monetary rewards.

SPMs depict brain regions engaged during the receipt of monetary rewards, visualized by performing a one-sample t-test on participants' WIN>NO CHANGE contrasts (time-locked to the onset of each trials' feedback phase). Images are presented at a threshold of $p(\text{FDR}) < 0.05$, $k > 10$). Left = Left, Right = Right. $N = 24$. Color bar indicates t-statistic value.



Supplementary Figure 8. Amphetamine-induced nucleus accumbens DA release and reward-related BOLD signal are positively correlated. Scatter plot shows that amphetamine-induced DA release in the right NAcc predicts a corresponding increase in reward anticipation-related right NAcc BOLD signal. Note that the correlation is still significant after removing two outlier subjects with negative % DA release values ($r = .57$, $p = 0.01$; one-tailed test).

Supplementary Data

Expanded striatal analysis

The study focused on the NAcc based on the rich preclinical literature on NAcc DA, drug abuse, and reward motivation. However, it is also important to determine whether the area of correlation was limited to the NAcc or reflected a larger pattern of heightened sensitivity throughout the striatum. To determine the specificity of our trait-imaging relationships to the NAcc as compared to other striatal regions, we examined PET and fMRI correlations with PPI-IA scores using an SPM approach in a search region that included the entire striatum (created using the caudate and putamen masks from the Anatomical Automatic Labeling atlas as implemented in the Wake Forest University PickAtlas), at an uncorrected threshold of $p < 0.001$. These analyses revealed a positive correlation between PPI-IA scores and amphetamine-induced DA release at an additional focus in the ventrolateral putamen (peak MNI coordinates: 28, 2, -2). No significant effects arose in dorsal areas of the striatum. No additional areas of activation outside of the nucleus accumbens were noted in the fMRI data. These data indicate that the association between mesolimbic DA responsivity and impulsive-antisocial traits may expand beyond the nucleus accumbens (at least as defined by the Harvard-Oxford atlas), but is limited to the ventral striatum.

Distribution of PPI scores

The distribution of psychopathic trait scores in our community sample is largely consistent with that seen in other community samples. To test this, we conducted independent samples t-tests on the PPI total score and each PPI subscale using our data and that reported in a larger community study by Blonigen et al (2003)(1). Out of these nine comparisons, three were statistically significant (median $t = 1.67$, corresponding to a p value of .095). While our sample's mean score on Coldheartedness was significantly lower than that of the Blonigen et al. (2003) sample, our sample's mean scores on Social

Potency and Fearlessness scales (which, along with the Stress Immunity scale, comprise the PPI-FD factor) were actually significantly higher than those in the Blonigen et al. (2003) sample. Crucially, our sample's means on the subscales comprising the PPI-IA factor were not significantly different from those of this much larger ($n = 353$) community sample.

Descriptive Statistics for NAcc D2/D3 Binding Potential Values

Descriptive statistics for baseline and post-amphetamine D2/D3 binding values in our NAcc region of interest were as follows. Right NAcc: $\text{Mean}_{\text{Baseline}} = 28.63$, $\text{SD}_{\text{Baseline}} = 3.49$; $\text{Mean}_{\text{Post-AMPH}} = 26.85$, $\text{SD}_{\text{Post-AMPH}} = 3.37$. Left NAcc: $\text{Mean}_{\text{Baseline}} = 28.83$, $\text{SD}_{\text{Baseline}} = 3.60$; $\text{Mean}_{\text{Post-AMPH}} = 26.95$, $\text{SD}_{\text{Post-AMPH}} = 3.17$). Repeated-Measures ANOVA confirmed a significant reduction in binding potential within the NAcc following the administration of amphetamine (Left NAcc: $p = 0.00003$; Right NAcc: $p = 0.00002$).

Correction for Multiple Correlation Tests

As multiple correlation tests were run between our brain imaging measures and different trait scores and subscores, we performed a Bonferroni correction on the p-values derived from our PET and fMRI analyses. For the both the PET and fMRI data, we chose an extremely conservative approach to correction that was based on three separate correlation tests (i.e. PPI-Total, PPI-IA, and PPI-FD) on two sides (left and right NAcc). This yields a corrected threshold of $p < 0.008$ ($.05/6$). The p-values for the correlation between PPI-IA and left and right NAcc DA release both survived this corrected threshold (left NAcc: $p = 0.003$; right NAcc: $p = 0.002$). The p-value for the correlation between PPI-IA and right NAcc BOLD signal survived this corrected threshold as well ($p = 0.001$).

PPI Total Score Correlations

In voxel-wise analyses, PPI Total scores were positively correlated with NAcc DA release at a trend level, but this correlation did not survive correction for multiple voxel-wise comparisons (Left NAcc: -12, 6, -14; $Z = 3.14$, $k = 29$, $p_{\text{FDR}} = 0.07$; Right NAcc: 20, 10, -10; $Z = 2.80$, $k = 44$, $p_{\text{FDR}} = 0.07$). PPI Total scores were also positively correlated with right NAcc BOLD signal at trend level, but this correlation did not survive correction for multiple correlation tests (Right NAcc: $r = 0.49$, $p = 0.02$).

Baseline-Controlled Analyses

To control for the possibility that our correlations between trait psychopathy and DA release were driven by differences in baseline D2/D3 receptor binding, we carried out a baseline-adjusted analysis of the impact of PPI-IA on AMPH-induced DA release in the NAcc. First, we performed a one-sample T-test to construct an SPM of the main effect of [18F]fallypride binding across subjects. We then masked this SPM with our anatomical NAcc region of interest and extracted baseline binding values for each subject from left and right NAcc. We confirmed via Pearson correlation analysis that there is no relationship between PPI-IA and D2/D3 baseline values ($p = 0.40$, right; $p = 0.31$, left), nor between PPI Total scores and D2/D3 baseline values ($p = 0.40$, right; $p = 0.33$, left) in this region. Next, the extracted baseline binding values were entered as a covariate of no interest in a multiple regression with NAcc DA-release as the dependent variable and PPI-IA a predictor of interest (i.e. an ANCOVA model). This analysis confirmed that the relationship between PPI-IA and amphetamine-induced DA release in the NAcc is still significant ($p = 0.0001$, right; $p = 0.00008$, left) even after accounting for NAcc D2/D3 baseline binding values.

Sex-by-Trait Interaction Analyses

Given known gender differences in the expression of psychopathy(2), we additionally tested for gender differences in the relationship between PPI-IA and our PET and fMRI measures of dopamine reward system function. While our PET sample was

relatively well balanced with respect to sex, our fMRI sample has significantly more women than men. This aspect of our study was not by design, but rather a consequence of the fact that our subject recruitment was agnostic with respect to sex. Given the higher prevalence of psychopathy in men, significant sex differences in the expression of the psychopathic phenotype, and the suggestion that the neural basis of psychopathy may differ between the sexes(2), the possibility of sex-specific associations between psychopathic traits and our measures of mesolimbic DA reward system function merited direct examination. To this end, we performed univariate general linear model analyses to explicitly examine whether sex interacts with trait psychopathy to influence NAcc amphetamine-induced DA release and reward anticipation-related BOLD signal. We constructed three separate models with right NAcc DA release, left NAcc DA release and right NAcc BOLD signal as dependent measures; sex, PPI-IA and a sex*PPI-IA interaction term were included as predictors in all models. For the PET data, PPI-IA emerged as the sole significant influence on NAcc amphetamine-induced DA release (right NAcc DA release: $p = 0.00002$; left NAcc DA release: $p = 0.00003$), suggesting the absence of a sex-by-trait interaction in this dataset (right NAcc DA release: $p = 0.14$; left NAcc DA release: $p = 0.1$).

Separate correlation analyses for men and women confirmed that PPI-IA scores were significantly correlated with NAcc DA release in both genders (Men: $r = 0.87$, $p = 0.00005$ [left NAcc]; $r = 0.76$, $p = 0.002$ [right NAcc]; Women: $r = .53$, $p = 0.03$ [left NAcc]; $r = .65$, $p = 0.006$). Using a Fisher Z-transform, we examined whether the correlation coefficients were significantly different between genders. For right NAcc, this difference was not significant ($z = 0.56$, $p = 0.58$; two-tailed test); however, this difference was significant at trend-level for left NAcc ($z = 1.89$, $p = 0.06$; two-tailed test), suggesting that PPI-IA may be modestly more predictive of left NAcc DA release in men compared to women.

For the fMRI data, the sex-by-trait interaction analysis revealed that PPI-IA was the sole significant predictor of right NAcc BOLD signal ($p = 0.001$). However, the sex-by-IA interaction term was significant at trend-level ($p = 0.06$). Sex-specific analyses confirmed that the relationship between PPI-IA and right NAcc BOLD signal was significant in both genders (Men: $r = 0.71$, $p = 0.047$; Women: $r = .68$, $p = 0.004$). A test for significant difference between these correlation coefficients was not significant ($z = 0.11$, $p = .91$; two-tailed test). This suggests that the slope of the PPI-IA-BOLD correlation is somewhat steeper in men compared to women, even though the effect size of PPI-IA on right NAcc BOLD signal is not significantly different between sexes.

On the whole, these results indicate that there is a similar relationship between NAcc functioning and impulsive-antisocial traits in both men and women, with weak evidence for somewhat stronger relationships in men compared to women. Studies with larger samples would be needed to test for these subtle effects.

Specificity of PPI-IA Trait Associations to Brain Measures: Control Analyses

Given that prior work has demonstrated that more general aspects of temperament – such as attentional/cognitive impulsivity, novelty seeking, and extraversion – also predict DA-linked aspects of brain function, including drug-induced ventral striatal DA release and/or BOLD signal responses to reward(3-9), we performed a series of control analyses to examine the specificity of our trait/brain imaging relationships to impulsive-antisociality. To control for potential effects due to attentional/cognitive and motor impulsivity, we performed a partial correlation analysis using participants scores on a trait measure of “pure” impulsivity, the Barratt Impulsiveness Scale-11 (BIS-11) (PET sample: Mean = 58.23, SEM = 1.81, Range = 43 to 84; fMRI sample: Mean = 59.29, SEM = 2.21, Range = 44 to 84). Correlations between PPI-IA and NAcc DA release were still significant after controlling for participants’ BIS-11 scores (r ’s = 0.59/0.56, p ’s = 0.001/0.002, left/right NAcc), as were the correlations between PPI-IA and NAcc

BOLD signal ($r = 0.56$, $p = 0.005$; right NAcc). Of note, the BIS-11 is particularly correlated with the PPI-IA subscale indexing cognitive impulsivity (correlation with Carefree Nonplanfulness subscale: $r = 0.76$, $p = 0.000000003$; combined sample of unique subjects, $N = 44$). If this cognitive impulsivity element of the PPI-IA factor drove the observed correlations between PPI-IA and NAcc neurochemistry and neurophysiology, there should be little association between PPI-IA and these measures after controlling for BIS-11 scores. The fact that DA release and BOLD signal correlations with PPI-IA remained highly significant after controlling for BIS-11 scores suggests that our observed trait-brain relationships were not driven by “mere” impulsivity *per se*, but rather reflect an influence of the more antisocial dimension of the impulsive-antisocial trait construct.

To control for potential effects due to novelty seeking and extraversion, we performed a partial correlation analysis using scores on the Novelty Seeking scale of the Tridimensional Personality Questionnaire (TPQ-NS; PET sample: Mean = 16.30, SEM = 0.73, Range = 9 to 28; fMRI sample: Mean = 15.61, SEM = 1.04, Range = 8 to 29) and the Extraversion scale of the NEO Personality Inventory-Revised (NEO-E; PET sample: Mean = 126.14, SEM = 2.91, Range = 90 to 166; fMRI sample: Mean = 121, SEM = 2.16, Range = 102 to 143). Correlations between PPI-IA and NAcc DA release remained significant even after controlling for novelty seeking and extraversion scores (r 's = 0.62/0.61, p 's = 0.0004/0.0004 [TPQ-NS], r 's = 0.67/0.67, p 's = 0.00009/0.00009 [NEO-E]). Correlations between PPI-IA and NAcc BOLD signal also remained significant after these partial correlation analyses ($r = 0.55$, $p = 0.008$ [TPQ-NS], $r = 0.55$, $p = 0.008$ [NEO-E]). Additionally, we used a multiple correlation approach within SPSS 17 to simultaneously assess the influence of PPI-IA, BIS-11, TPQ-NS and NEO-E scores on extracted left and right NAcc DA release values and BOLD signal values. For AMPH-induced DA release, PPI-IA still emerged as a significant predictor of AMPH-induced

DA release ($p = 0.004$, right; $p = 0.002$, left), even after simultaneously adjusting for BIS-11, TPQ-NS and NEO-E scores. PPI-IA also emerged as a significant predictor of right NAcc BOLD signal ($p = 0.01$) even after simultaneously adjusting for BIS-11, TPQ-NS, and NEO-E scores.

Associations between psychopathic traits and brain activity during reward feedback

Of note, no significant relationships were found between either PPI-IA or PPI-FD and BOLD signal during the reward feedback phase of the task in either the NAcc (right NAcc: PPI-IA, $r = 0.07$, $p = 0.74$; PPI-FD, $r = -0.01$, $p = 0.96$; Left NAcc: PPI-IA, $r = 0.01$, $p = 0.96$; PPI-FD, $r = -0.03$, $p = 0.91$) or in the medial prefrontal cortex (mPFC; see Supplementary Methods) (PPI-IA: $r = 0.05$, $p = 0.83$; PPI-FD: $r = -0.05$, $p = 0.82$). These data indicate that NAcc information processing is selectively biased toward the anticipation of rewards in individuals with high levels of IA traits, but not FD traits.

Supplementary Discussion

In the current study, we utilized a dimensional measure of psychopathic traits in a community sample of individuals with no history of substance abuse. While not identical to studying incarcerated criminal psychopaths, this approach avoids the serious confound of substance abuse, which is typically present in studies of incarcerated psychopaths. The validity of using trait measures to assess psychopathy is supported by recent findings that delineate a dimensional, rather than taxonomic, structure for this construct(10, 11). The dimensional nature of psychopathy, which implies the presence of a continuous distribution of psychopathic traits within the general population(12), makes tenable an approach to studying the neurobiological basis of the disorder that utilizes community sampling in concert with trait measures of psychopathy. Critically, such measures significantly predict antisocial behavior and substance abuse in unincarcerated community samples(13-16) and aggressive misconduct and clinical diagnosis of psychopathy in incarcerated samples (17, 18), supporting the assertion that they assess

core elements of the psychopathy construct. Further, while participants in the current study did not meet criteria for Axis-I psychiatric disorders, in all other regards they are essentially an unselected sample of community volunteers. Importantly, the distribution of psychopathic trait scores in our community sample is largely consistent with that seen in other community samples (*1*)(see Supplementary Data above). Thus, although not directly measured, our high scoring participants presumably show the same propensity for maladaptive behaviors (with the exception of substance abuse) as high scorers in other community samples.

In considering the relationship between psychopathy specifically and antisocial behavior more generally, we note that it is widely held that the emotional/interpersonal features of psychopathy distinguish it from other forms of antisocial psychopathology (such as DSM-IV defined Antisocial Personality Disorder; APD). While it is true that the emotional and interpersonal dimensions contribute to the distinctiveness of psychopathy compared to APD, socially deviant behavior is still central to the construct and measurement of psychopathy. For example, Factor 1 (emotional/interpersonal) and Factor 2 (antisocial lifestyle) items are given equal weight in scoring the “gold standard” of psychopathy measurement, the Psychopathy Checklist-Revised; PCL-R. On the whole, our selective association between measures of mesolimbic DA reward system function and impulsive-antisocial traits (which are more strongly linked to the antisocial lifestyle component of psychopathy), and our observed lack of association between fearless-dominance traits (which are more strongly linked to the emotional/interpersonal component of psychopathy) suggests that enhanced mesolimbic DA function may be involved in the more broad antisocial lifestyle domain that is common to both psychopathy and APD. It is interesting in this regard that some researchers have previously distinguished between “primary” and “secondary” psychopathy, with secondary psychopaths being characterized by impulsive aggression and criminal

behavior, but normal or above normal physiological responses to threat (in contrast to primary psychopaths, who characteristically lack anxiety and fearfulness). Consistent with our present findings, it has been theorized that these secondary psychopaths have excessive activity within Gray's so-called Behavioral Activation System (part of a conceptual model of the nervous system involved in approach behavior) (19, 20).

In the present study, we have proposed the hypothesis that neurochemical and neurophysiological hypersensitivity to reinforcers within the mesolimbic DA system may promote the development of persistent aggression in parallel with its putative influence on substance abuse susceptibility. This hypothesis suggests that factors that predispose enhanced stimulated DA release or diminished DA clearance should influence risk for impulsive-aggressive phenotypes. Supporting this notion, low-expressing polymorphic variants of DA catabolic enzyme and transporter genes that are associated with enhanced striatal responsivity to reward have also been linked to aggression and addiction(4, 21, 22). Of note, the pattern of stimulant-induced DA release seen in the present study mirrors that of healthy subjects who possess other temperamental risk factors for addiction. For example, high novelty-seeking subjects with no prior history of psychostimulant use show exaggerated stimulant-induced DA release (5). Further, Alia-Klein and colleagues have found that diminished striatal monoamine oxidase A (MAO-A) activity – which presumably results in elevated striatal DA levels – predicts increased trait aggression in healthy subjects(23). In addition, early life stress - a significant environmental risk factor for both aggression and substance abuse – sensitizes adult mesolimbic DA function in animal models(24). These prior studies raise the intriguing possibility that the mesolimbic DA reward system may be a common neurobiological vulnerability nexus that is sensitive to the influence of diverse risk factors for socially deviant behavior. The current findings converge to further implicate increased human

NAcc dopaminergic transmission and reward-based information processing in the pathophysiology of risk for antisocial psychopathology.

Supplementary Methods

Participants

Participants were studied as part of an ongoing investigation of individual differences in striatal and extrastriatal DA release. All participants were medically and psychiatrically healthy adults, age 18 to 35, with estimated IQ greater than 80. Subjects were excluded if they had any history of substance abuse, current tobacco use, alcohol intake greater than 8 ounces of whiskey or equivalent per week, use of psychostimulants (excluding caffeine) more than twice in the subject's lifetime or at all in past 6 months, any psychotropic medication for the past 6 months other than occasional use of benzodiazepines for sleep, history of psychiatric illness, significant medical condition, any condition which would interfere with MRI or PET studies (e.g., extreme obesity, claustrophobia, cochlear implant, metal fragments in eyes, cardiac pacemaker, neural stimulator, and metallic body inclusions or other metal implanted in the body which may interfere with MRI scanning, pregnancy, anemia). Urine drug screens were used to confirm current abstinence from drugs of abuse. Additionally, some participants were scanned with fMRI without having undergone PET scanning. Exclusion criteria for these subjects were similar to those described above, but relied exclusively on self-report (i.e., no SCID or urine drug screen was performed, but participants completed a brief questionnaire covering current and past psychopathology and substance abuse).

Following initial screening, subjects were given an interview of their medical history and a structured psychiatric interview (SCID-NP). In addition to the regular questions in the non-alcohol substance dependence section of the SCID-NP, subjects were asked to indicate the number of times that they have taken any drug that they indicate having tried. They were also asked whether or not they had taken the drug within

the last 2 months. Subjects were excluded if they had taken cocaine or amphetamines more than once in their life. Any illicit drug use in the last 2 months was grounds for exclusion, even in subjects who did not otherwise meet criteria for substance abuse. Urine drug screens were performed to test for the presence of amphetamines, cocaine, marijuana, PCP, and opiates, benzodiazepines, and barbiturates.

All subjects with available data were included in each analysis. 30 subjects had both PET and PPI data (15 male, 15 female). 24 subjects had both fMRI and PPI data (8 male, 16 female). Of these 24 fMRI subjects, 10 also completed PET scans, while the remaining 14 were scanned with fMRI only. An additional 8 participants completed PET and fMRI scanning, but were scanned prior to the inclusion of the PPI in the respective studies. These subjects were included in analysis of PET-fMRI correlations but not in any other analyses.

Personality Measures

PPI: To assess psychopathic traits, we used the Psychopathic Personality Inventory (PPI)(16). The PPI comprises of 187 multiple-choice items that are answered according to a 4-point Likert scale (1 = *false*, 2 = *mostly false*, 3 = *mostly true*, 4 = *true*). The PPI yields a total score, as well as scores for eight subscales: Impulsive Nonconformity (17 items), Blame Externalization (18 items), Machiavellian Egocentricity (30 items), Carefree Nonplanfulness (20 items), Stress Immunity (11 items), Social Potency (24 items), Fearlessness (19 items), and Coldheartedness (21 items). In addition, the PPI contains 10 “Deviant Responding” items designed to detect random responses or malingering, and 14 “Unlikely Virtues” items designed to index social desirability.

Each of the above subscales access specific constituent elements within the psychopathic trait domain. Based on the work of Lilienfeld, Benning, and other investigators (13, 16), a picture of high scoring individuals on each of these subscales has emerged. According to these descriptions, high scorers on the Impulsive Nonconformity

scale are reckless, rebellious, and unconventional; high scorers on the Blame Externalization scale blame others for their own problems and rationalize their own transgressions; high scorers on the Machiavellian Egocentricity scale are aggressive, narcissistic and exploitative; high scorers on the Carefree Nonplanfulness scale lack forethought and planning; high scorers on the Stress Immunity scale experience minimal anxiety and show attenuated emotional reactions to anxiogenic situations and stimuli; high scorers on the Fearlessness scale are less sensitive to potentially harmful outcomes for actions; and high scorers on the Coldheartedness scale are callous and unsentimental.

Full-scale scores were obtained by summing subscale scores for each participant. Benning and colleagues used principal axis factor analysis to identify two higher order factors(13). This analysis demonstrated distinct factor loadings for PPI subscales. Based on this work, we constructed PPI-FD factor scores by summing z-scores for the Social Potency, Stress Immunity, and Fearlessness subscales. For the PET sample, mean, SEM, and range for each of these scales were: 67.17, 2.02, 44-85 (Social Potency); 32.90, 0.99, 15-39 (Stress Immunity); and 48.43, 2.13, 27-74 (Fearlessness). For the fMRI sample, mean, SEM and range for each of these scales were: 63.83, 1.82, 44-79 (Social Potency); 32.08, 1.18, 15-39 (Stress Immunity); and 50.58, 1.77, 35-71(Fearlessness). PPI-IA factor scores were obtained by summing z-scores for the Machiavellian Egocentricity, Blame Externalization, Carefree Nonplanfulness, and Impulsive Nonconformity subscales. For the PET sample, mean, SEM and range for each of these scales were: 61.13, 2.06, 45-89 (Machiavellian Egocentricity); 28.10, 1.12, 19-39 (Blame Externalization); 34.93, 1.27, 23-55 (Carefree Nonplanfulness); and 34.57, 1.54, 22-57 (Impulsive Nonconformity). For the fMRI sample, mean, SEM and range for each of these scales were: 64.21, 2.69, 45-93 (Machiavellian Egocentricity); 29.17, 1.39, 19-41 (Blame Externalization); 37.83, 1.63, 27-60 (Carefree Nonplanfulness); and 35.83, 1.89, 24-52 (Impulsive Nonconformity).

Additional measures: In order to assess whether the correlations with the PPI might be

better explained by other nonspecific personality traits, we additionally assessed several general personality domains that are conceptually linked to psychopathy or dopamine functioning. To assess cognitive/attentional and motor impulsivity, we used the Barratt Impulsiveness Scale, version 11 (BIS-11), one of the most widely used measures of impulsive personality traits. The BIS-11 is a 30 item self-report questionnaire, which yields scores for 9 factors and a full-scale score. We used full-scale scores only for our partial correlation analyses. To assess extraversion, we used the extraversion scale of the Revised NEO Personality Inventory (NEO PI-R). The NEO PI-R is a 240 item self-report measure of the Five Factor Model of personality, comprised of Extraversion, Agreeableness, Conscientiousness, Neuroticism, and Openness to Experience. To assess novelty seeking, we used the novelty seeking scale of the Tridimensional Personality Questionnaire, a 100 item self-report questionnaire that gives scores on three scales (Harm Avoidance, Novelty Seeking, Reward Dependence), each with four subscales. For partial correlation and multiple regression analyses, we used full-scale scores on the Extraversion and Novelty Seeking scales.

PET

Image Acquisition and Analysis: All PET images were acquired using [^{18}F]fallypride. [^{18}F]Fallypride ((*S*)-*N*-[(1-allyl-2-pyrrolidinyl)methyl]-5-(3[^{18}F]fluoropropyl)-2,3-dimethoxybenzamide) is a substituted benzamide with very high affinity to D2/D3 receptors(25). Unlike other D2/D3 ligands, [^{18}F]fallypride allows stable estimates of D2-like binding in both striatal and extrastriatal regions(26). [^{18}F]Fallypride has also been found to be sensitive to endogenous DA release (27), particularly in the striatum, making it an ideal ligand for use in conjunction with a dual scan strategy that allows assessment of both baseline receptor availability and individual differences in induced DA release.

Protocols for PET image acquisition and analysis were derived from a larger ongoing study and have been previously published (28, 29). Subjects received two PET

scans using [^{18}F]fallypride. The first scan was a baseline placebo scan; the second scan was performed while the subject received an amphetamine (d-AMPH) challenge. PET imaging was performed on a GE Discovery LS scanner located at Vanderbilt University Medical Center that was upgraded to a Discovery STE system during the course of the study. All subjects received their baseline and d-AMPH scans on the same scanner. To ensure the validity of combining data across scanners, we performed a voxel-wise analysis comparing DA release between the two scanners. No clusters survived whole brain correction at $t=2.5$ (lowest cluster-level $p\text{-value} > .90$). Moreover, no differences were observed in our NAcc anatomical region-of-interest (ROI). Both scanners had an axial resolution of 4 mm, and in-plane resolution of 4.5-5.5 mm FWHM at the center of the field of view. [^{18}F]fallypride was produced in the radiochemistry laboratory attached to the PET unit, following synthesis and quality control procedures described in US Food and Drug Administration IND 47,245. Scans were timed to start 3 hours after 0.43mg/kg oral d-AMPH administration, which was timed to coincide with the period of peak plasma d-AMPH. 3-D emission acquisitions scans were performed following a 5.0 mCi slow bolus injection of [^{18}F] Fallypride (specific activity greater than 3000 Ci/mmol). Serial scans were started simultaneously with the bolus injection of [^{18}F] Fallypride and were obtained for approximately 3.5 hours, with two 15-minute breaks for subject comfort. Transmission scans were collected for attenuation correction prior to each of the three emission scans.

Binding Potential Maps: Each subject's serial PET scans were first corrected for motion across scanning periods and then co-registered to the subject's structural T1-weighted MRI image (28). Regional D2/D3 binding potential (nondisplaceable) was calculated on a voxelwise basis using the full reference region method(30), with cerebellum chosen as the reference region because of its relative lack of D2/D3 receptors(31). Voxelwise kinetic modeling was executed using Interactive Data Language (RSI, Boulder, CO). Prior studies in our lab indicate that the reference region method produces binding potential estimates

that are in close agreement with estimates derived from Logan plots (32) using a metabolite corrected plasma input function. Because [^{18}F] Fallypride binding values exhibit significant variability across different regions (e.g., striatum vs. PFC), we used variance estimates at the voxelwise level rather than the pooled variance used in typical parametric analyses (33). Because the inherent resolution of the Fallypride PET scans is fairly smooth relative to the size of the nucleus accumbens, we did not perform any additional spatial smoothing. Prior to group analyses, a composite binding potential and PET image was created, and warped to a template MRI. The transformation matrix from this warping was then applied to the binding potential maps in order to bring all subjects data into a common space (MNI space). Individual images of voxelwise percent-change in binding between placebo and amphetamine scans (representing DA release) were calculated for each subject by subtracting amphetamine scan binding potential images from placebo scan binding potential images. These “placebo-corrected” images were then divided by placebo scan binding potential images to create a map of percent-change (after multiplying each voxel value by 100) in each voxel of [^{18}F]fallypride binding (i.e. percent change in DA release due to amphetamine administration).

Group Correlation Maps: Group analyses of the PET data were performed in SPM5 by regressing subjects’ PPI Total and factor scores on their percent-change DA release images. Analyses for PPI-FD, PPI-IA, and PPI Full-scale scores were conducted separately. In all cases, gender was included as a covariate. Multiple regression statistical parametric maps (SPMs) were masked with a nucleus accumbens (NAcc) region of interest (ROI), obtained from the Harvard-Oxford atlas in FSL (<http://www.fmrib.ox.ac.uk/fsl/>). The Harvard-Oxford atlas provides a probabilistic definition of the NAcc in MNI space based on a semi-automated segmentation of 38 healthy subjects (<http://www.fmrib.ox.ac.uk/fsl/fslview/atlas-descriptions.html#ho>). We note that the NAcc as defined in the Harvard-Oxford atlas provides a general boundary of the NAcc that does

not incorporate individual differences in the precise topographic boundaries of the region. However, because such subtle topographical boundaries cannot be detected with MRI or PET, the application of a standardized mask provides the most reliable and replicable approach to defining the NAcc across subjects. SPMs were thresholded at $p < 0.05$; cluster threshold was set to 10 contiguous voxels. Only voxels surviving False Discovery Rate correction for multiple comparisons ($p < 0.05$) within the NAcc ROI are reported.

fMRI

Monetary Incentive Delay Task: Details of the MID task have been published previously (34). Briefly, participants had the opportunity to win or lose money by pressing a button during the very brief presentation of visual target stimulus. The MID task session consisted of 180 6-s trials. During each trial, participants were shown one of seven cues (cue phase, 1s), indicating that they had the potential to win money (WIN trials; amount = \$0.20, \$1 or \$5; $n = 74$), that they had the potential to lose money (LOSE trials; amount = \$0.20, \$1 or \$5; $n = 69$), or that no money was at stake for that trial (NO CHANGE trials; $n = 37$). Participants then fixated on a cross-hair during a variable interval (anticipatory delay phase, 2000–2500 ms), and finally responded to a white target square that appeared for a variable length of time (target phase, 160–260 ms) with a button press. For WIN trials, participants were told that if they successfully pressed the button while the target was onscreen (a “hit”) they won the amount of money indicated by the cue, while there was no penalty for failing to press the button while the target was onscreen (a “miss”). For LOSE trials, participants were told that no money was won or lost for hits, but misses led to a loss of the amount indicated by the cue for that trial. Critically, by contrasting brain activations in the anticipatory delay phase in WIN trials vs. NO CHANGE trials it is possible to examine the extent to which the anticipation of potential reward modulates ventral striatal activity during this preparatory period. A feedback screen (outcome phase, 1650 ms) followed the target's disappearance. The

feedback screen notified participants how much money they won or lost during that trial, and indicated their cumulative total winnings at that point. A variable inter-trial interval of between 3 and 6 seconds separated each trial. fMRI volume acquisitions were time-locked to the offset of each cue and each target, so were thus acquired during anticipatory and during outcome periods. Even though no money was at stake during the NO CHANGE trials, participants were instructed to rapidly press the button during the display of the target stimulus. Before entering the scanner, participants completed a practice version of the task and were shown the money that they could earn by performing the task successfully. Based on reaction times obtained during the prescan practice session, target durations were adjusted such that each participant succeeded on approximately 66% of his or her responses. Each MID task session was comprised of 4 functional runs, each approximately 7.73 minutes long.

MRI Scanning: All fMRI scans were performed on two identically configured 3 Tesla Phillips Achieva scanners located at the Vanderbilt University Institute for Imaging Science (VUIIS). The MID was programmed in E-Prime (<http://www.pstnet.com/products/e-prime/>) and run off of a dedicated Pentium computer from the scanner control room. The visual display was presented on an LCD panel and back-projected onto a screen positioned at the front of the magnet bore. Subjects lay supine in the scanner and viewed the display on a mirror positioned above them. Manual responses were recorded using a keypad (Rowland Institute of Science, Cambridge MA).

Functional scans: Functional (T2* weighted) images were acquired using a gradient-echo echoplanar imaging (EPI) pulse sequence with the following parameters: TR 2000 ms, TE 25 ms, flip angle 90°, FOV 240x240mm, 128x128 matrix with 30 axial oblique slices (2.5 mm, .25mm gap) oriented approximately 15 degrees from the AC-PC line. The slice prescription was adjusted for each subject to ensure coverage of the midbrain, ventral striatum, amygdala, medial prefrontal cortex and orbital gyrus. Higher-order

shimming was employed to compensate for magnetic field inhomogeneity in the orbitofrontal/ventral striatal region. 242 volumes were acquired for each functional run.

Anatomical scans: T1-weighted high-resolution 3D anatomical scans were obtained for each participant (FOV 256x256, 1x1x1mm resolution). In addition, fast spin echo axial spin density weighted (TE=19, TR=5000, 3 mm thick) and T2-weighted (TE=106, TR=5000, 3 mm thick) slices were obtained to exclude any structural abnormalities. Additionally, a field map was collected in order to remove distortion caused by magnetic field inhomogeneity.

Preprocessing: Prior to random effects analysis in SPM5, functional images were slice-time corrected using the middle slice as a reference, and motion corrected via spatial realignment (4th degree B-spline) of all images to a mean image after alignment to the first image of each run. Following realignment, the Fieldmap toolbox was used to create voxel displacement maps (VDMs) from static magnetic field (B0) maps acquired during each scan session. These VDMs were used to correct for susceptibility-X-movement-related distortions in the EPI images. These distortion-corrected images were then co-registered to the subject's anatomical image. Images were spatially normalized (4th degree B-spline) into a standard stereotactic space (MNI template), resampled into 2mm isotropic voxels, and smoothed with a 6mm full-width-half-maximum gaussian kernel. We then applied a high-pass filter (128s cutoff) to remove low-frequency signal drift. Each subject's data were inspected for excessive motion – only subjects with <3mm motion in every direction across all runs were included in analyses.

Single-subject SPMs: All win trials and all lose trials (across all monetary values), and all no change trials were pooled. Onsets for the anticipatory delay period and for the feedback period of each of the three trial types were separately modeled using a canonical hemodynamic response function (HRF) with a time derivative. In addition, six head

motion parameter estimates (translation in x,y,z; roll, pitch, yaw) were included as covariates in the design matrix. Each run was modeled separately.

Group analyses: Group analyses of the fMRI data were performed as follows. First, using the MarsBar toolbox within SPM5(35), we extracted BOLD signal estimates and calculated percent-change in BOLD signal for each condition (i.e. averaged across all trials of a given condition) for each subject averaged across all voxels contained in the right and left anatomical NAcc regions of interest derived from the Harvard-Oxford Probabilistic atlas. Percent-change values for No Change (Delay) trials were subtracted from Win (Delay) trials. We then separately correlated each subject's left and right NAcc BOLD signal percent-change values with their PPI-FD, PPI-IA, and PPI Full-scale scores using a two-tailed Pearson correlation within SPSS 17. Differences in subject sex and scanner were controlled using a two-tailed partial correlation within SPSS 17 ($r = 0.63$, $p = 0.002$, for the correlation between PPI-IA and right NAcc BOLD). To test the influence of psychopathic traits on medial prefrontal cortex activity during reward feedback, we extracted BOLD percent-change values for each subject for each condition from a medial prefrontal cortex (mPFC) region of interest derived from a random-effects main effect map of the contrast Win (Feedback) > No Change (Feedback) (see Supplementary Figure 4). Percent-change values for No Change (Feedback) trials were subtracted from Win (Feedback) trials. We then separately correlated each subject's mPFC BOLD signal percent-change values with their PPI-FD, PPI-IA, and PPI Full-scale scores using a two-tailed Pearson correlation within SPSS 17. Finally, we examined the relationship between psychopathic traits and NAcc activation during reward feedback by calculating BOLD signal percent change values with the NAcc ROI as above (i.e. percent-change values for Win[Feedback] trials – percent-change values for No Change[Feedback] trials) and correlating these with PPI-FD, PPI-IA, and PPI Full-scale scores via two-tailed Pearson correlation within SPSS 17

Additional Statistical Analyses

fMRI-PET Correlations

To assess the relationship between PET and fMRI signal in the NAcc, we extracted BOLD signal estimates from a right NAcc region of interest constructed from the PPI-IA/DA-release correlation map (masked using the Harvard-Oxford right NAcc anatomical region of interest at an uncorrected threshold of $p < 0.05$). Percent-change contrast values for Win (Delay) > Win (No Change) were constructed as described above for each subject. These values were then correlated with each subject's percent-change DA value, which was extracted from a random-effects main effect map of DA release (masked using the Harvard-Oxford right NAcc anatomical region of interest at an uncorrected threshold of $p < 0.05$) using a one-tailed Pearson correlation within SPSS 17. The one-tailed test was justified by our a-priori hypothesis of a significant positive relationship between NAcc DA release and BOLD signal.

Partial Correlation Analyses

Two-tailed partial correlations and multiple correlations between NAcc DA release and BOLD signal estimates and PPI-IA, BIS-11, TPQ-NS and NEO-E scores were carried out in SPSS 17, with $\alpha = 0.05$. Sex was included as an additional covariate for all analyses, and for partial correlation and multiple regression analysis of BOLD signal within SPSS, scanner was included as a covariate as well. Regarding these analyses, it is not our intention to suggest that individual differences in “pure” impulsivity, Novelty Seeking, and/or Extraversion (measured by the BIS-11, TPQ-NS and NEO-E) are unrelated to individual differences in NAcc dopamine signaling and/or anticipatory reward processing. Rather, these analyses demonstrate that the observed positive correlations between the Impulsive-Antisociality factor of the PPI (PPI-IA) and amphetamine-induced NAcc DA release and reward-related NAcc BOLD signal in our sample cannot be accounted for by interindividual variation in these other variables. Our

partial correlation and multiple regression analyses do not demonstrate that PPI-IA is linked to NAcc dopamine *to the exclusion of these other variables*.

1. D. M. Blonigen, S. R. Carlson, R. F. Krueger, C. J. Patrick, *Personality and Individual Differences* **35**, 179 (2003).
2. E. M. Cale, S. O. Lilienfeld, *Clin Psychol Rev* **22**, 1179 (Nov, 2002).
3. I. Boileau *et al.*, *Arch Gen Psychiatry* **63**, 1386 (Dec, 2006).
4. E. E. Forbes *et al.*, *Mol Psychiatry* **14**, 60 (Jan, 2009).
5. M. Leyton *et al.*, *Neuropsychopharmacology* **27**, 1027 (Dec, 2002).
6. A. R. Hariri *et al.*, *J Neurosci* **26**, 13213 (Dec 20, 2006).
7. M. X. Cohen, J. Young, J. M. Baek, C. Kessler, C. Ranganath, *Brain Res Cogn Brain Res* **25**, 851 (Dec, 2005).
8. R. Cools, M. Sheridan, E. Jacobs, M. D'Esposito, *J Neurosci* **27**, 5506 (May 16, 2007).
9. R. A. Depue, P. F. Collins, *Behav Brain Sci* **22**, 491 (Jun, 1999).
10. J. P. Guay, J. Ruscio, R. A. Knight, R. D. Hare, *J Abnorm Psychol* **116**, 701 (Nov, 2007).
11. J. F. Edens, D. K. Marcus, S. O. Lilienfeld, N. G. Poythress, Jr., *J Abnorm Psychol* **115**, 131 (Feb, 2006).
12. R. D. Hare, C. S. Neumann, *Annu Rev Clin Psychol* **4**, 217 (2008).
13. S. D. Benning, C. J. Patrick, B. M. Hicks, D. M. Blonigen, R. F. Krueger, *Psychol Assess* **15**, 340 (Sep, 2003).
14. C. S. Neumann, R. D. Hare, *J Consult Clin Psychol* **76**, 893 (Oct, 2008).
15. K. M. Schmeelk, P. Sylvers, S. O. Lilienfeld, *J Pers Disord* **22**, 269 (Jun, 2008).
16. S. O. Lilienfeld, B. P. Andrews, *J Pers Assess* **66**, 488 (Jun, 1996).
17. J. F. Edens, N. G. Poythress, S. O. Lilienfeld, C. J. Patrick, A. Test, *Psychol Assess* **20**, 86 (Mar, 2008).
18. J. F. Edens, N. G. Poythress, Jr., S. O. Lilienfeld, C. J. Patrick, *Behav Sci Law* **26**, 529 (2008).
19. D. T. Lykken, *The Antisocial Personalities*. (Lawrence Erlbaum Associates, Hilldale, New Jersey, 1995).

20. J. P. Newman, D. G. MacCoon, L. J. Vaugh, N. Sadeh, *Journal of Abnormal Psychology* **114**, 319 (2005).
21. J. C. Dreher, P. Kohn, B. Kolachana, D. R. Weinberger, K. F. Berman, *Proc Natl Acad Sci U S A* **106**, 617 (Jan 13, 2009).
22. J. Volavka, R. Bilder, K. Nolan, *Ann N Y Acad Sci* **1036**, 393 (Dec, 2004).
23. N. Alia-Klein *et al.*, *J Neurosci* **28**, 5099 (May 7, 2008).
24. P. Kehoe, W. J. Shoemaker, L. Triano, J. Hoffman, C. Arons, *Behav Neurosci* **110**, 1435 (Dec, 1996).
25. J. Mukherjee, Z. Y. Yang, M. K. Das, T. Brown, *Nucl Med Biol* **22**, 283 (Apr, 1995).
26. B. T. Christian *et al.*, *J Cereb Blood Flow Metab* **24**, 309 (Mar, 2004).
27. M. Slifstein *et al.*, *Synapse* **54**, 46 (Oct, 2004).
28. P. Riccardi *et al.*, *Neuropsychopharmacology* **31**, 1016 (May, 2006).
29. D. H. Zald *et al.*, *J Neurosci* **28**, 14372 (Dec 31, 2008).
30. A. A. Lammertsma, S. P. Hume, *Neuroimage* **4**, 153 (Dec, 1996).
31. H. Hall *et al.*, *Neuropsychopharmacology* **11**, 245 (Dec, 1994).
32. J. Logan *et al.*, *J Cereb Blood Flow Metab* **10**, 740 (Sep, 1990).
33. A. Dagher *et al.*, in *Quantitative Functional Brain Imaging with Positron Emission Tomography*, R. Carson, M. Daube-Witherspoon, P. Herscovitch, Eds. (Academic Press, London, 1998).
34. B. Knutson, G. W. Fong, C. M. Adams, J. L. Varner, D. Hommer, *Neuroreport* **12**, 3683 (Dec 4, 2001).
35. M. Brett, J.-L. Anton, R. Valabregue, J. B. Poline, paper presented at the International Conference on Functional Mapping of the Human Brain, Sendai, Japan, 2002.